Int J Coal Sci Technol (2017) 4(3):281–299
DOI 10.1007/s40789-017-0178-x

Identification of nitrogen-polyaromatic compounds in asphaltene from co-processing of coal and petroleum residue using chromatography with mass spectrometry

Pingping Zuo[1] · **Wenzhong Shen**[1]

Received: 21 March 2017 / Revised: 25 June 2017 / Accepted: 17 July 2017 / Published online: 28 July 2017

Abstract Asphaltene, from co-processing of coal and petroleum residues is one of the most precious and complex molecular mixtures existing, with tremendous economic relevance. Asphaltene was separated by Soxhlet extraction with methylbenzene and then divided into three parts by distillation. Gas chromatography (GC) and high-performance liquid chromatography (HPLC) were coupled with quadrupole time-of-flight mass spectrometry (Q-TOF MS) to separate and characterize organic nitrogen species in the distillates of asphaltene at molecular level. Molecular mass of compounds was mainly distributed from 150 to 600 μ. Number of rings plus double bonds (rdb) and synchronous fluorescence spectra indicated that most of the organonitrogen compounds (NPAC) contained heterocyclic aromatic rings, including pyridines, anilines, quinolins, pyrroles, carbazoles and indoles plus various alkyl groups. Constant-wavelength synchronous fluorescence spectrometry (CWSFS) indicated NPAC with 2–3 rings were the main structures of organonitrogen compounds and the corresponding structural information was proposed. Some organic nitrogen isomers were separated and identified by atmospheric pressure chemical ionization (APCI) GC-Q-TOF MS and electrospray ionization (ESI) HPLC-Q-TOF MS. The methodology applied here contained chromatographic injection of the diluted sample using conventional columns sets and Data Analysis 4.2 software. Identifying molecular structures provides a foundation to understand all aspects of coal-derived asphaltene, enabling a first-principles approach to optimize resource utilization.

Keywords Co-processing of coal and petroleum residue · Asphlatene · Heterocyclic aromatic rings · GC-Q-TOF MS · HPLC-FL-Q-TOF MS

1 Introduction

Co-processing of coal and petroleum residues is a promising way for converting coal and petroleum residues into oil and an amount of residues. The content of asphaltene in residues is up to 40%, it is an important precursor to gasification, synthesis carbon materials and asphalt. As complex mixture, it is difficult to separate and identify of composite of asphaltene (Zhang et al. 2002; Ying et al. 2009; Xu et al. 2013). In fact, asphaltene, which is rich in aromatic compounds such as polycyclic aromatic hydrocarbons (PAHs) and believed as the polar fraction, has the N, O, S atoms, some of which substitute the carbon in the aromatic chain normally (Gargiulo et al. 2016). Soxhlet extraction, a nondestructive separation technique, can well separate and enrich compounds with similar solubility and polarity from a mixture. Generally, the residues components are separated into several fractions based on the different solubility in *n*-hexane (*n*-heptane), tetrahydrofuran (THF) and toluene. The composition that can be dissolved in benzene or toluene-soluble but undissolved in alkanes-insoluble fraction is defined as asphaltene (Mullins et al. 2012; Wu and Kessler 2015). While the complexity compounds cannot be represented by a single model or representative structure and required accurate perspectives

---

✉ Wenzhong Shen
shenwzh2000@yahoo.com

[1] State Key Laboratory of Coal Conversion, Institute of Coal Chemistry, Chinese Academy of Sciences, Taiyuan 030001, People's Republic of China

distributions and structural features of these residues. One of the most important, understanding the modes of occurrence and distribution of heteroatoms in residues is also necessary for potential application.

N-polyaromatic compounds is widely existed in coal and petroleum residues, it could be used as photoconductors, semiconductors (Plater and Jackson 2003) and they are valuable constituents of pharmacologically active synthetic compounds and agrochemical intermediates (Li et al. 2015; Matzke et al. 2015; Gargiulo et al. 2016). N-polyaromatic compounds (NPAC) generally were classified into two types: neutral pyrrolic and basic pyridinic. The neutral organonitrogen consists of indole, pyrrole, carbazole and their alkylated analogues, while the basic organonitrogen contains pyridines, quinolines, benzoquinolines and their alkylated analogues (da Silva et al. 2014). Thus, it is essential to characterize these structures in order to understand their roles and behaviors, also to find effective approaches to separate and effectively utilize.

GC coupled to different mass spectrometry detectors, including GC-Q-TOF MS, has been proven a powerful tool to separate and analyze complex components in the complex fuel-derived mixtures, such as coal tars, pitches, and petroleum asphaltenes, especially for lower molecular-mass (MM) components (Beens et al. 2000; Barman et al. 2001; da Silva et al. 2014).

The majority of the compounds in asphaltene are not volatile enough for GC analysis, HPLC–MS is a better choice with higher molecular mass, and/or lower thermal stability. Reversed-phase (RP) LC accompanied by ESI is commonly used for investigation of polar compounds, like NPAC. It was reported that isomers in beeswax and in coal could be separated and identified using HPLC with PAH column in CH_3OH system (Ares et al. 2015; You et al. 2015). These compounds in asphaltene were usually detected by UV or diode array (Smith et al. 2009; Zubkova 2011), fluorescence (George et al. 2010; Zubkova 2011) (FL) and MS detectors (Smith et al. 2009). Researchers (Wang et al. 2013) speculated that coal asphaltene liquefied at different temperatures consisted of similar aromatic structure, mainly 2–3 rings condensed nucleuses, by UV–Vis absorption spectra of coal asphaltene in THF solvent. CWSFS, which differs from the common fluorescence method and scans excitation wavelength and emission wavelength synchronously, is widely used to elucidate the fundamental properties of polycyclic aromatic hydrocarbons of complex mixtures like asphaltenes (Goncalves et al. 2004; Abdallah and Yang 2012; Pereira et al. 2014; Wu and Kessler 2015). It has better selectivity, higher sensitivity and less interference than UV–Vis absorption spectra. CWSFS presents the size of aromatic nucleuses of asphlatenes, and the increase of asphaltene aromaticity leads to the increase of fluorescence intensity. Fluorescence spectroscopy is not a very sensitive method, containing fluorophore (George et al. 2010). Sometimes deviation exists when molecular diameter of the asphaltene is measured by Fluorescence depolarization (FD) study (Abdallah and Yang 2012). With high qualitative ability and mass accuracy, Time-of-flight mass (TOF) analyzer can well separate and identify the elemental composition and chemical information, including carbon number, heteroatom content and isotopic distributions. Polar molecules (polar heteroatomic species, basic compounds with quinolones and pyridines rings) could be ionized by ESI source; while lower polarity molecules and neutral nitrogen species with pyrroles, indoles and carbazoles rings could be ionized by APCI source. Roussis et al. who first directly measured high-molecular-weight petroleum compounds reported bimodal asphaltene molecular weights of $300 < m/z < 20{,}000$ using a hybrid magnetic sector–TOF tandem mass spectrometer (McKenna et al. 2013). However, there are many isomers with monomeric molecular weight and molecular aggregation in asphaltene, it is difficult to characterize these molecules by MS analysis.

In this work, the GC-APCI-Q-TOF MS and HPLC-FL-ESI-Q-TOF MS were applied in the speciation of NPAC of asphaltene derived from co-processing coal and oil residues. The asphaltene was subjected to distillation instead of column chromatography which was normally complex and the attendant risk of sample loss (da Silva et al. 2014). We also got several cleaner mass spectra to verify the isomers. Analytical information such as retention times, *m*/*z*, error, msiga as well as rdb was used to identify the compounds. Fluorescence spectra were complementary to predict the aromatic structures of asphlatene that were mainly inferred by the rdb values.

2 Materials and methods

2.1 Chemicals and sample

Coal sample was collected from Shenfu coal mine. Petroleum slurry was from Shijiazhuang Refining & Chemical. THF, hexane and methylbenzene were commercial analytical reagents supplied from Sinopharm (China) and were further distilled before use. Methanol and acetonitrile were purchased from Thermo Fisher scientific (USA) with purity above 99.9%.

2.2 Preparation of asphalene distillates

The co-processing of coal and oil slurry with a weight ratio of 1:1 was operated at 450 °C and in the pressure of 8 MPa in N_2 for 8 h (Wu et al. 2012), and the resultant residue was named COR. COR was treated with hexane for 2 h and then insoluble substance was extracted with THF by Soxhlet extraction for 8 h. The THF-soluble fraction, called asphalt, was obtained by reduced pressure distillation after removing THF. Asphaltene was got finally by extracting asphalt in methylbenzene with Soxhlet extractor for 8 h and then separated into three parts according to distillation range: fraction a (<100 °C), fraction b (100–200 °C) and fraction c (>200 °C). The fractions were centrifuged and then diluted with methanol before analysis, shown as Fig. 1.

3 Characterizations

3.1 GC-APCI-Q-TOF MS spectrometry

The fraction a and b were analyzed by GC-APCI-Q-TOF MS system, which was performed with a GC-650 (Bruker, German) and a Q-TOF MS spectrometer (Bruker, German) equipped with APCI source. The column set was formed by BR-5ms capillary column (selectivity similar to 5% diphenyl/95% dimethyl polysiloxane) with 30 m length, 0.25 mm internal diameter and 0.25 μm film thickness (Bruker, German). The carrier gas was nitrogen at a flow rate of 1 mL/min. The injection was achieved at 250 °C with a 1:200 split ratio and an injection volume of 1.0 μL. The temperature was kept at 50 °C for 2 min and reached 300 °C at 8 °C/min and for 10 min. In the APCI source, nebulizer pressure, capillary voltage, dry heater, and flow rate of dry gas were set to 3.0 bar, 3000 V, 250 °C and 2.5 L/min, respectively. Data were collected over a mass range of 50–500 Daltons.

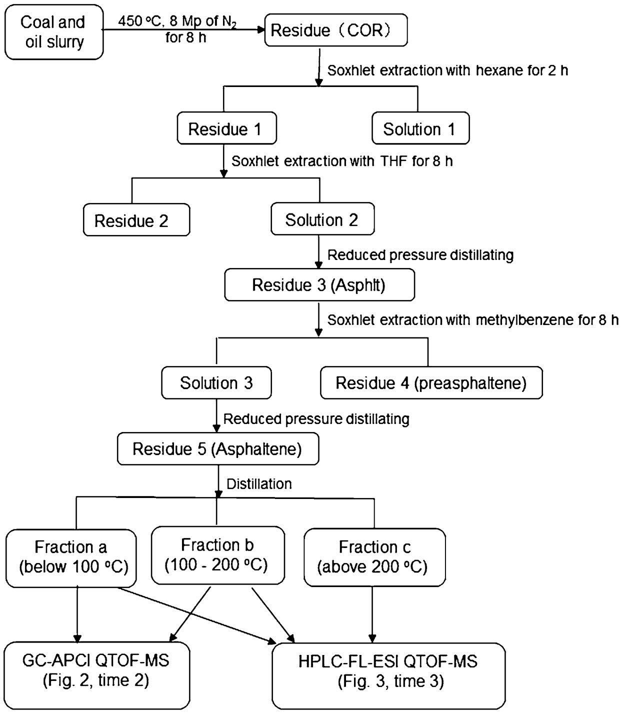

Fig. 1 The experimental procedure

3.2 HPLC-FL-ESI-QTOF-MS spectrometry

All distillates, a, b and c, were analyzed by an HPLC (Thermo, USA)-fluorescence spectrophotometer (HITACHI F-7000, Japan)-ESI-QTOF-MS. Samples (5 μL) were injected into the HPLC equipped with a Zorbax PAH column (4.6 mm id × 25 mm; 5 μm particle size, Agilent, USA) by an autosampler with a 0.5 mL/min isocratic elution (80:20 methanol/water) flow rate, and temperature of the column was maintained at 25 °C.

CWSFS was operated as follow: the spectrometer was set to scan at a rate of 240 nm/min with a slit width of 5 nm. Synchronous spectra covered a 240–500 nm range at a constant wavelength difference of 14 nm between emission and excitation wavelengths. PMT voltage was 400 V.

In the ESI source, capillary voltage, nebulizer pressure, dry heater, and flow rate of dry gas were set to 4500 V, 2.0 bar, 350 °C, 220 °C and 10 L/min, respectively. The separated analytes were monitored by the Q-TOF-MS with m/z from 50 to 1000 μ in positive ion mode.

Elemental Analysis was operated on elemental analyzer (vario M-CUBE, Germany).

4 Results and discussion

4.1 Analysis by double bond equivalence and fluorescence spectra

Asphaltene produced by co-processing of coal and oil slurry accounted for more than 80% (weight percentage) of asphalt, the amount of nitrogen in this asphaltene is about 0.7% which is relatively low compared to coal (varying from 1% to 2%) (Barman et al. 2001; da Silva et al. 2014), many N-polyaromatic compounds were tentatively identified of which mass spectral fragmentation patterns are very unique and easily identified.

Species were detected as protonated molecules: $[M + H]^+$ ion both in Figs. 2 and 3. Figure 2a, b showed the APCI (+)-Q-TOF MS results for fraction a and b separated by GC. Figure 3a–c showed the ESI (+)-Q-TOF MS spectra of fraction a, b and c separated by HPLC, respectively. More than one hundred peeks were detected, sometimes chromatographic separation was not efficient, but the simultaneous sampling mode and the process of spectral deconvolution of Q-TOF MS produced a mass spectrum more reliable than those produced by scanning mass analyzers, like quadrupole analyzer. Several

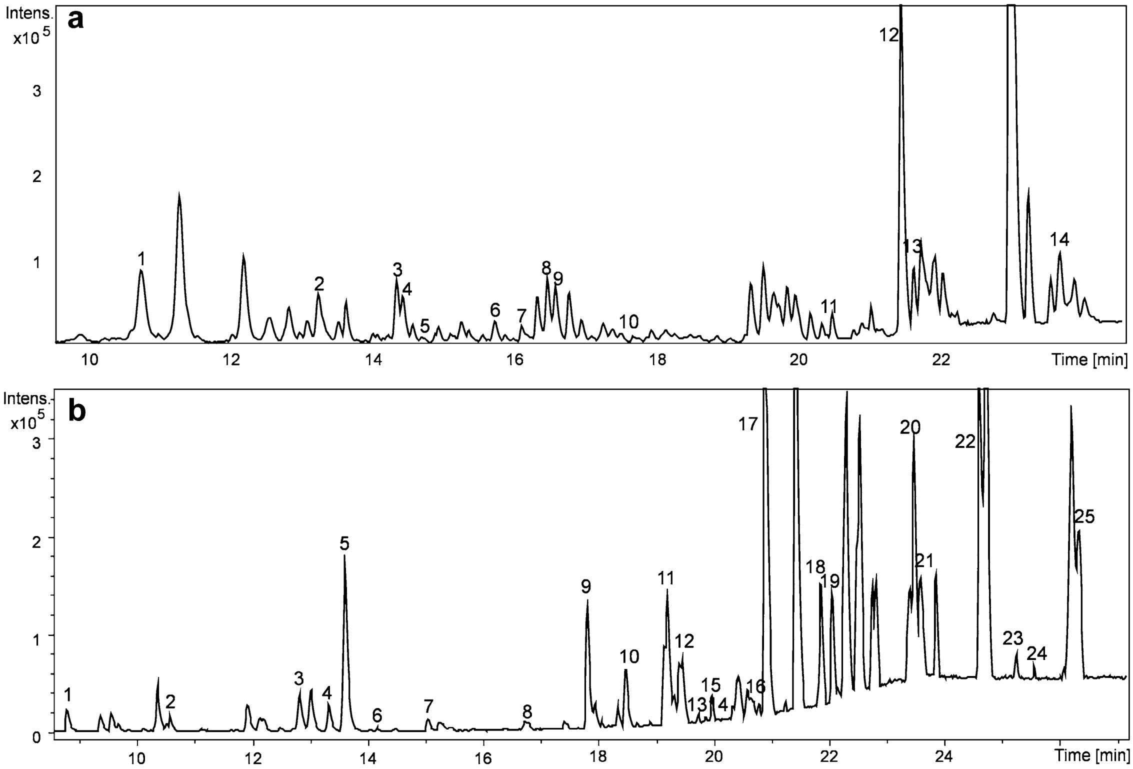

Fig. 2 The Base Peak Chromatogram (BPC) of fraction a and b analyzed by GC-APCI-MS, fourteen peaks were identified in **a** and twenty-five peaks were identified in **b**. Some compounds may flow out at same time

compounds may flow out at same time in MS spectra, the paper focused on the compounds with relatively high intensity.

The molecular-mass of N-containing compounds in asphaltene were mainly from 150 to 600 μ. The high resolution mass Base Peak Chromatogram (BPC) spectra offered accurate ion molecular formulas ($[M + H]^+$). The ion molecular formula was limited to a maximum numbers for 5 Nitrogen, 2 Sulfur, and 10 Oxygen. The identification of compounds was mainly based on the follow parameters: retention times, ion formula ($[M + H]^+$), measured *m/z* (Meas. *m/z*), deviation between measured mass and theoretical mass of the selected peak ([mDa]) and mSigma. MSigma is a rate describing how well the theoretical isotopic peaks match to the sample isotopic peaks. Generally, the values were set as <5 mDa for deviation and <100 for mSigma, the lower was the better. Table 1 only showed the tentatively identified N-compounds of the minimum deviation and mSigma processed using the Data Analysis 4.2 software. For instance, $[C_{16}H_{12}N]^+$ ($m/z = 218.0964$) was detected at 24.7 min with mDa = 1.1 and mSigma = 1.9 in Fig. 2b, at 18.2 min with mDa = 1.3 and mSigma = 88.9 in Fig. 3a, 23.7 min with mDa = 1.4 and mSigma = 41.2 in Fig. 3b, at 24.4 min with mDa = 0.1 and mSigma = 8.8 in Fig. 3c, respectively. Table 1 only showed the last set of data in comprehensive consideration of deviation and mSigma. The composition of compound is expressed by the class of chemical formula such as $C_xH_yN_\beta O_\alpha S_\gamma$. Rdb is calculated from the number of atoms and their valency indicating the degree of unsaturation for molecules. The valences of C, N, O, S and H were assumed as 4, 3, 2, 2 and 1, respectively, as follow:

$$R + db = \frac{2 + \sum n(atom) \times (valency - 2)}{2}$$

Each double bond or naphthene increases one rdb number and eliminates two hydrogen atoms, and every increment of three rdb units results in an additional aromatic ring fused to an aromatic core (Xia et al. 2016). Table 1 listed the rdb of $[M + H]^+$, and $rdb\ (M) = rdb\ ([M + H]^+) + 0.5$.

The rdb of compound was combined with its CWSFS to predict the structure. As nondestructive method, Fluorescence spectroscopy was used to compare the relative sizes of aromatic ring systems of the samples separated by HPLC. The conjugated π bonds of compounds resulted in a marked shift to longer wavelengths in their fluorescence spectra. Meanwhile, the fluorescence efficiency increases significantly with the increase of aromatic rings. In consideration of the "red shift" effect caused by alkylation and heteroatom, the numbers of aromatic rings of the compounds were summarized as follows: 270–300 nm for

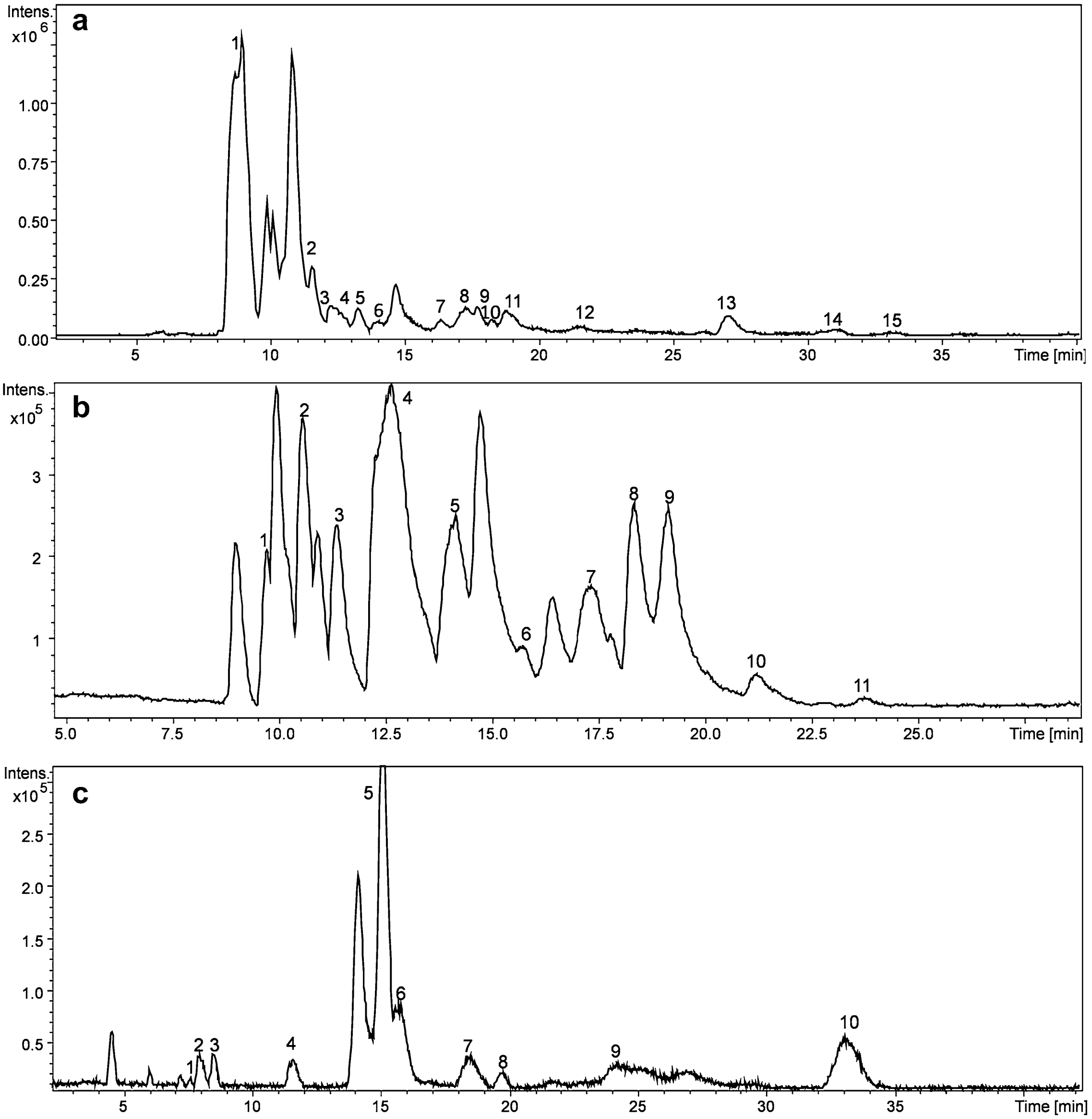

Fig. 3 The BPC of fraction a, b and c analyzed by HPLC–ESI–MS, fifteen, eleven and ten peeks were identified, respectively. Some compounds may flow out at same time

single-ringed aromatics, 300–340 nm for double-ringed aromatics, 340–400 nm for three aromatic rings, 400–425 nm for four aromatic rings, lager than 425 nm for five- and above five-ringed aromatics (Michels et al. 1996).

In $N_1O_\alpha S_\gamma$ ($\alpha + \gamma \leq 2$) group, since the minimum rdb of $[M + H]^+$ for pyridines is 3.5, compounds with rdb < 3.5 are possible amines. The species with rdb = 3.5 may be pyridines or anilines. The ones with rdb = 4.5 may be pyridines/anilines/benzene linked an aliphatic ring or an unsaturated group. The ones with rdb = 5.5 may contain an aromatic ring and aliphatic rings and/or unsaturated groups. The compounds with rdb = 6.5 may be quinolones. Figure 2a showed the MS result of part of fraction a with lower polarity and ionized by APCI. Specifically, $[C_9H_8N]^+$ appeared at 10.3 min with rdb = 6.5 was presumed to be quinolone; $[C_{16}H_{34}NO]^+$ (at 14.4 min) with rdb = 0.5 and $[C_{25}H_{50}NO_2]^+$ (at 23.5 min) with rdb = 1.5 possibly contained an amino-group. Figure 2b presented the MS result of part of fraction b also with lower polarity and ionized by APCI. For example, $[C_{12}H_{26}NO]^+$ (at 8.0 min), $[C_7H_{16}NS_2]^+$ (at 19.1 min), $[C_9H_{18}NS_2]^+$ (at 20.0 min), $[C_{18}H_{36}NO]^+$ (at 23.5 min), of which rdb was smaller than 3.5, may be O- or S- aliphatic amines; $[C_{14}H_{22}NOS]^+$ detected at 19.7 min with rdb = 4.5 may contain a pyridine/thiophene/phenyl ring with substituent group. Figure 3 showed the MS results of part of fraction a, b and c with polarity and ionized by ESI. More specifically, saturated amines were detected in Fig. 3a, as $[C_8H_{20}NS_2]^+$

Table 1 Tentatively N-compounds identified in Figs. 2 and 3

No.	Time 2 (min)		Time 3 (min)			Meas. *m*/*z*	Ion formula $[M + H]^+$	|err| [mDa]	mSigma	rdb of $[M + H]^+$
	2-a GC	2-b GC	3a LC	3b LC	3c LC					
1	10.3					130.0649	C_9H_8N	0.2	4.2	6.5
2			12.5			144.0822	$C_{10}H_{10}N$	1.4	10.1	6.5
3				12.7		156.0808	$C_{11}H_{10}N$	0.0	37.3	7.5
4			16.4			158.0972	$C_{11}H_{12}N$	0.8	14.3	6.5
5				17.3		164.1433	$C_{11}H_{18}N$	0.1	13.6	3.5
6		18.5				168.0801	$C_{12}H_{10}N$	0.7	19.2	8.5
7			14.0			170.0961	$C_{12}H_{12}N$	0.3	14.1	7.5
8				15.8		172.112	$C_{12}H_{14}N$	0.1	16.3	6.5
9					19.7	180.0815	$C_{13}H_{10}N$	0.7	5.8	9.5
10		19.9				182.0955	$C_{13}H_{12}N$	1.0	5.9	8.5
11		16.7				184.1168	$C_{13}H_{14}N$	4.7	12.8	7.5
12				21.2		194.0966	$C_{14}H_{12}N$	0.1	29.3	9.5
13		20.9				196.1097	$C_{14}H_{14}N$	2.4	9.2	8.5
14		21.8				204.0791	$C_{15}H_{10}N$	1.6	5.2	11.5
15			16.4			206.0987	$C_{15}H_{12}N$	2.3	77.4	10.5
16			21.4			208.1134	$C_{15}H_{14}N$	1.4	66.0	9.5
17					24.4	218.0963	$C_{16}H_{12}N$	0.1	8.8	11.5
18					46.5	230.0975	$C_{17}H_{12}N$	1.1	12.1	12.5
19		26.3				232.1102	$C_{17}H_{14}N$	1.9	3.0	11.5
20		24.6				244.118	$C_{18}H_{14}N$	4.9	64.9	12.5
21			31.1			254.0979	$C_{19}H_{12}N$	1.5	19.9	14.5
22				9.8		138.092	$C_8H_{12}NO$	0.7	28.8	3.5
23				10.6		142.1229	$C_8H_{16}NO$	0.3	28.3	1.5
24					7.7	158.1544	$C_9H_{20}NO$	0.5	28.0	0.5
25					7.7	180.1341	$C_{11}H_{18}NO$	4.2	6.3	3.5
26		8.0				200.1996	$C_{12}H_{26}NO$	1.3	50.0	0.5
27				12.7		196.0758	$C_{13}H_{10}NO$	0.2	75.2	9.5
28				14.1		210.0913	$C_{14}H_{12}NO$	0.0	8.7	9.5
29					7.7	222.088	$C_{15}H_{12}NO$	3.3	81.8	10.5
30					11.6	232.0748	$C_{16}H_{10}NO$	0.9	57.9	12.5
31	14.4					256.2617	$C_{16}H_{34}NO$	1.8	1.5	0.5
32	14.3					246.0907	$C_{17}H_{12}NO$	0.6	29.1	12.5
33		19.4				252.139	$C_{17}H_{18}NO$	0.7	16.1	9.5
34		23.5				282.2777	$C_{18}H_{36}NO$	1.4	32.4	1.5
35			21.4			274.1245	$C_{19}H_{16}NO$	1.9	58.7	12.5
36			13.3			314.1588	$C_{22}H_{20}NO$	4.9	50.6	13.5
37			13.3			432.2366	$C_{31}H_{30}NO$	4.4	35.2	17.5
38				11.4		130.067	$C_6H_{12}NS$	1.5	41.3	1.5
39				14.1		144.0821	$C_7H_{14}NS$	2.0	18.0	1.5
40				12.7		156.0808	$C_8H_{14}NS$	3.4	58.3	2.5
41			11.7			158.0984	$C_8H_{16}NS$	1.4	15.1	1.5
42			14.0			170.0961	$C_9H_{16}NS$	3.7	29.1	2.5
43			16.4			172.1123	$C_9H_{18}NS$	3.1	29.1	1.5
44					14.9	180.082	$C_{10}H_{14}NS$	2.1	8.3	4.5
45			16.4			194.0985	$C_{11}H_{16}NS$	1.2	46.3	4.5
46					33.0	204.082	$C_{12}H_{14}NS$	4.9	24.9	6.5

Table 1 continued

No.	Time 2 (min)		Time 3 (min)			Meas. *m*/*z*	Ion formula $[M + H]^+$	|err| [mDa]	mSigma	rdb of $[M + H]^+$
	2-a GC	2-b GC	3a LC	3b LC	3c LC					
47			16.4			206.0987	$C_{12}H_{16}NS$	1.1	83.3	5.5
48				21.2		208.1115	$C_{12}H_{18}NS$	3.9	16.9	4.5
49			21.4			218.0982	$C_{13}H_{16}NS$	1.5	33.0	6.5
50			17.1			220.1108	$C_{13}H_{18}NS$	4.7	90.8	5.5
51			21.4			230.099	$C_{14}H_{16}NS$	0.7	29.1	7.5
52			31.1			254.0979	$C_{16}H_{16}NS$	1.9	40.2	9.5
53			33.0			218.2134	$C_{12}H_{28}NO_2$	2.0	17.3	−0.5
54			12.5			368.1693	$C_{25}H_{22}NO_2$	4.8	30.1	15.5
55	23.5					396.3811	$C_{25}H_{50}NO_2$	2.5	72.7	1.5
56			13.3			382.185	$C_{26}H_{24}NO_2$	4.8	66.6	15.5
57		19.1				178.0757	$C_7H_{16}NS_2$	3.9	42.1	0.5
58			16.4			194.0985	$C_8H_{20}NS_2$	4.6	63.6	−0.5
59		20.0				204.092	$C_9H_{18}NS_2$	4.5	57.5	1.5
60		19.7				252.139	$C_{14}H_{22}NOS$	2.7	37.4	4.5
61			13.3			432.2366	$C_{28}H_{34}NOS$	1.0	52.7	12.5
62			12.5			368.1693	$C_{22}H_{26}NO_2S$	1.4	8.0	10.5
63			11.7			368.1694	$C_{22}H_{26}NO_2S$	1.5	49.5	10.5
64			13.3			382.185	$C_{23}H_{28}NO_2S$	1.4	64.4	10.5
65			13.3			432.2366	$C_{25}H_{38}NOS_2$	2.4	75.3	7.5
66				21.2		338.2355	$C_{19}H_{32}NO_4$	2.9	40.9	4.5
67			12.5			440.1892	$C_{28}H_{26}NO_4$	3.6	34.1	16.5
68			12.5			368.1693	$C_{19}H_{30}NO_2S_2$	1.9	22.6	5.5
69			13.3			382.185	$C_{20}H_{32}NO_2S_2$	1.9	71.1	5.5
70					7.9	195.0929	$C_{13}H_{11}N_2$	1.2	34.8	9.5
71			13.3			219.0913	$C_{15}H_{11}N_2$	0.4	59.3	11.5
72			8.7			231.0872	$C_{16}H_{11}N_2$	4.5	37.9	12.5
73		25.2				259.1237	$C_{18}H_{15}N_2$	0.7	14.3	12.5
74					15.6	261.1362	$C_{18}H_{17}N_2$	2.5	11.6	11.5
75	21.6					303.2804	$C_{20}H_{35}N_2$	0.9	15.9	4.5
76	10.3					313.26	$C_{21}H_{33}N_2$	3.8	19.1	6.5
77	10.3					341.2924	$C_{23}H_{37}N_2$	2.7	43.6	6.5
78	21.4					511.5016	$C_{35}H_{63}N_2$	3.0	61.0	5.5
79	14.3					199.091	$C_{12}H_{11}N_2O$	4.4	27.6	8.5
80	15.7					213.1067	$C_{13}H_{13}N_2O$	4.4	7.7	8.5
81			14.0			305.1664	$C_{20}H_{21}N_2O$	1.5	56.0	11.5
82				19.1		355.2782	$C_{23}H_{35}N_2O$	3.8	20.5	7.5
83	10.3					359.303	$C_{23}H_{39}N_2O$	2.7	75.9	5.5
84			8.7			143.0682	$C_6H_{11}N_2S$	4.5	28.0	2.5
85	14.3					155.0678	$C_7H_{11}N_2S$	4.1	31.2	3.5
86				11.4		181.0824	$C_9H_{13}N_2S$	3.0	18.0	4.5
87					7.9	195.0929	$C_{10}H_{15}N_2S$	2.2	56.8	4.5
88			17.1			355.1301	$C_{23}H_{19}N_2S$	3.8	40.9	15.5
89				15.8		365.1074	$C_{24}H_{17}N_2S$	3.3	79.6	17.5
90			13.3			409.1774	$C_{27}H_{25}N_2S$	4.1	46.8	16.5
91		13.3				155.0844	$C_7H_{11}N_2O_2$	2.9	35.8	3.5
92	8.9					157.0966	$C_7H_{13}N_2O_2$	0.5	41.3	2.5

Table 1 continued

No.	Time 2 (min)		Time 3 (min)			Meas. *m/z*	Ion formula $[M + H]^+$	$\lvert err \rvert$ [mDa]	mSigma	rdb of $[M + H]^+$
	2-a GC	2-b GC	3a LC	3b LC	3c LC					
93	10.3					163.1404	$C_7H_{19}N_2O_2$	3.7	81.5	−0.5
94		15.1				167.0843	$C_8H_{11}N_2O_2$	2.8	28.2	4.5
95		12.8				175.1469	$C_8H_{19}N_2O_2$	2.8	28.7	0.5
96	16.3					177.1577	$C_8H_{21}N_2O_2$	2.1	63.6	−0.5
97		19.1				179.0833	$C_9H_{11}N_2O_2$	1.8	74.7	5.5
98	13.1					191.1732	$C_9H_{23}N_2O_2$	2.2	17.5	−0.5
99		17.8				191.0839	$C_{10}H_{11}N_2O_2$	2.4	35.6	6.5
100	14.3					215.0846	$C_{12}H_{11}N_2O_2$	3.1	8.6	8.5
101		22.0				217.0997	$C_{12}H_{13}N_2O_2$	2.6	12.4	7.5
102		20.0				219.1136	$C_{12}H_{15}N_2O_2$	0.8	40.6	6.5
103		21.9				221.1296	$C_{12}H_{17}N_2O_2$	1.1	49.5	5.5
104	16.3					233.2186	$C_{12}H_{29}N_2O_2$	3.8	27.7	−0.5
105		23.4				233.1294	$C_{13}H_{17}N_2O_2$	0.9	64.9	6.5
106		23.5				247.2352	$C_{13}H_{31}N_2O_2$	1.1	34.1	−0.5
107	14.6					246.099	$C_{14}H_{13}N_2O_2$	1.9	21.5	9.5
108		25.2				245.1268	$C_{14}H_{17}N_2O_2$	1.7	47.6	7.5
109		25.2				247.1454	$C_{14}H_{19}N_2O_2$	1.3	40.0	6.5
110		25.3				311.2659	$C_{18}H_{35}N_2O_2$	3.4	8.7	2.5
111				23.7		399.2992	$C_{25}H_{39}N_2O_2$	1.4	49.8	7.5
112					8.5	413.1283	$C_{28}H_{17}N_2O_2$	0.2	49.8	21.5
113					14.9	579.2988	$C_{40}H_{39}N_2O_2$	1.8	35.9	22.5
114			18.2			355.1308	$C_{20}H_{23}N_2S_2$	1.1	46.3	10.5
115			27.1			361.1805	$C_{20}H_{29}N_2S_2$	3.8	97.8	7.5
116			13.3			409.1774	$C_{24}H_{29}N_2S_2$	0.7	66.3	11.5
117			21.4			413.2124	$C_{24}H_{33}N_2S_2$	4.4	72.4	9.5
118			27.1			463.226	$C_{28}H_{35}N_2S_2$	2.4	20.6	12.5
119				19.1		355.2782	$C_{20}H_{39}N_2OS$	0.4	38.2	2.5
120				23.7		391.2821	$C_{23}H_{39}N_2OS$	4.4	42.2	5.5
121			16.4			455.2201	$C_{29}H_{31}N_2OS$	4.9	85.9	15.5
122		13.6				161.0956	$C_6H_{13}N_2O_3$	3.5	32.5	1.5
123		19.4				207.0793	$C_{10}H_{11}N_2O_3$	2.9	98.6	6.5
124	21.6					333.315	$C_{18}H_{41}N_2O_3$	3.8	70.7	−0.5
125	23.5					375.356	$C_{21}H_{47}N_2O_3$	2.1	82.5	−0.5
126				23.7		365.1349	$C_{21}H_{21}N_2O_2S$	3.1	39.5	12.5
127					8.5	413.1283	$C_{25}H_{21}N_2O_2S$	3.6	55.6	16.5
128	16.4					445.1034	$C_{28}H_{17}N_2O_2S$	2.8	78.2	21.5
129			13.3			453.1678	$C_{28}H_{25}N_2O_2S$	4.7	66.7	17.5
130			18.7			465.1681	$C_{29}H_{25}N_2O_2S$	5.0	63.8	18.5
131			17.8			449.1734	$C_{26}H_{29}N_2OS_2$	1.9	67.6	13.5
132			16.4			455.2201	$C_{26}H_{35}N_2OS_2$	1.5	99.1	10.5
133			27.1			425.1746	$C_{24}H_{29}N_2OS_2$	3.0	70.9	11.5
134			31.1			659.2909	$C_{44}H_{39}N_2O_4$	0.4	37.4	26.5
135				21.2		365.1348	$C_{18}H_{25}N_2O_2S_2$	0.4	59.6	7.5
136			13.3			453.1678	$C_{25}H_{29}N_2O_2S_2$	1.3	42.9	12.5
137			18.7			465.1681	$C_{26}H_{29}N_2O_2S_2$	1.6	67.8	13.5
138				23.7		365.1349	$C_{17}H_{21}N_2O_7$	0.6	34.8	8.5

Table 1 continued

No.	Time 2 (min)		Time 3 (min)			Meas. *m*/*z*	Ion formula [M + H]$^+$	|err| [mDa]	mSigma	rdb of [M + H]$^+$
	2-a GC	2-b GC	3a LC	3b LC	3c LC					
139			13.3			415.2117	$C_{19}H_{31}N_2O_8$	4.2	31.7	5.5
140			13.3			437.1948	$C_{21}H_{29}N_2O_8$	3.0	29.1	8.5
141			33.0			463.2266	$C_{20}H_{35}N_2O_{10}$	2.0	41.3	4.5
142			13.3			409.1774	$C_{23}H_{25}N_2O_5$	1.6	33.4	12.5
143			27.1			425.1746	$C_{23}H_{25}N_2O_6$	3.9	28.6	12.5
144			13.3			453.1678	$C_{24}H_{25}N_2O_7$	2.2	72.4	13.5
145			18.7			465.1681	$C_{25}H_{25}N_2O_7$	2.5	29.3	14.5
146			16.4			455.2201	$C_{25}H_{31}N_2O_6$	2.4	87.8	11.5
147			33.0			463.2266	$C_{27}H_{31}N_2O_5$	3.9	27.9	13.5
148				18.3		579.2915	$C_{29}H_{43}N_2O_{10}$	0.3	10.4	9.5
149			16.4			158.0972	$C_6H_{12}N_3O_2$	4.8	13.4	2.5
150		23.4				210.0897	$C_9H_{12}N_3O_3$	2.4	47.3	5.5
151					18.5	206.094	$C_{10}H_{12}N_3O_2$	1.6	36.1	6.5
152	17.5					311.318	$C_{18}H_{39}N_4$	1.1	16.0	1.5
153					15.1	301.1435	$C_{19}H_{17}N_4$	1.1	6.1	13.5
154	20.5					353.3638	$C_{21}H_{45}N_4$	0.0	17.1	1.5
155			27.1			345.2063	$C_{22}H_{25}N_4$	1.1	9.4	12.5
156	16.1					365.3642	$C_{22}H_{45}N_4$	0.3	24.0	2.5
157	17.5					377.3634	$C_{23}H_{45}N_4$	0.5	20.4	3.5
158			18.7			375.16	$C_{25}H_{19}N_4$	0.4	36.4	18.5
159	21.6					449.457	$C_{28}H_{57}N_4$	0.7	23.5	2.5
160			27.1			425.1746	$C_{29}H_{21}N_4$	1.5	60.4	21.5
161			17.8			449.1734	$C_{31}H_{21}N_4$	2.6	16.2	23.5
162			16.4			455.2201	$C_{31}H_{27}N_4$	3.0	35.0	20.5
163			12.5			337.1997	$C_{20}H_{25}N_4O$	2.6	39.5	10.5
164	16.1					351.3119	$C_{20}H_{39}N_4O$	0.1	90.6	3.5
165	21.6					353.3321	$C_{20}H_{41}N_4O$	4.6	9.9	2.5
166	23.5					381.3629	$C_{22}H_{45}N_4O$	4.1	24.3	2.5
167				23.7		365.1349	$C_{23}H_{17}N_4O$	4.8	23.5	17.5
168	23.5					395.3783	$C_{23}H_{47}N_4O$	3.9	10.6	2.5
169	20.5					421.3913	$C_{25}H_{49}N_4O$	1.2	13.4	3.5
170			18.7			465.1681	$C_{31}H_{21}N_4O$	2.9	56.2	23.5
171			18.7			375.16	$C_{22}H_{23}N_4S$	3.8	29.6	13.5
172			27.1			425.1746	$C_{26}H_{25}N_4S$	4.9	56.6	16.5
173			13.3			415.2117	$C_{25}H_{27}N_4O_2$	1.1	22.0	14.5
174			13.3			437.1948	$C_{27}H_{25}N_4O_2$	2.4	11.2	17.5
175			31.1			371.2049	$C_{20}H_{27}N_4O_3$	2.8	54.7	9.5
176				23.7		467.1114	$C_{29}H_{15}N_4O_3$	2.5	36.6	24.5
177					14.9	579.2988	$C_{35}H_{39}N_4O_4$	2.2	18.6	18.5
178			31.1			659.2909	$C_{39}H_{39}N_4O_6$	4.4	13.4	22.5
179					14.9	579.2988	$C_{28}H_{43}N_4O_9$	3.7	33.1	9.5
180			12.5			440.1892	$C_{22}H_{26}N_5O_5$	3.6	4.2	12.5
181	8.9					338.3281	$C_{19}H_{40}N_5$	0.3	12.6	2.5
182				17.3		338.2364	$C_{20}H_{28}N_5$	2.5	34.7	9.5
183			12.3			440.1887	$C_{29}H_{22}N_5$	1.7	46.0	21.5
184	20.5					380.3409	$C_{21}H_{42}N_5O$	2.6	18.5	3.5

Table 1 continued

No.	Time 2 (min)		Time 3 (min)			Meas. *m/z*	Ion formula $[M + H]^+$	|err| [mDa]	mSigma	rdb of $[M + H]^+$
	2-a GC	2-b GC	3a LC	3b LC	3c LC					
185			12.5			440.1892	$C_{26}H_{26}N_5S$	1.1	40.2	16.5
186			12.5			440.1892	$C_{23}H_{30}N_5S_2$	4.5	66.7	11.5
187			13.3			432.2366	$C_{25}H_{30}N_5O_2$	2.8	45.8	13.5
188				23.7		365.1349	$C_{18}H_{17}N_6O_3$	0.8	23.0	13.5
189			13.3			437.1948	$C_{22}H_{25}N_6O_4$	1.6	15.9	13.5
190			27.1			425.1746	$C_{24}H_{21}N_6O_2$	2.5	35.6	17.5
191	23.5					396.3811	$C_{21}H_{46}N_7$	0.2	58.8	2.5
192			13.3			415.2117	$C_{20}H_{35}N_2O_3S_2$	3.4	28.0	4.5
193			13.3			409.1774	$C_{20}H_{29}N_2O_5S$	1.8	52.1	7.5
194			27.1			425.1746	$C_{20}H_{29}N_2O_6S$	0.5	42.7	7.5
195				23.7		467.1114	$C_{20}H_{23}N_2O_9S$	0.5	52.6	10.5
196			13.3			453.1678	$C_{18}H_{33}N_2O_7S_2$	4.6	30.0	3.5
197			18.7			465.1681	$C_{19}H_{33}N_2O_7S_2$	4.2	67.5	4.5
198			13.3			453.1678	$C_{21}H_{29}N_2O_7S$	1.2	49.8	8.5
199			18.7			465.1681	$C_{22}H_{29}N_2O_7S$	0.9	46.5	9.5
200			12.3			440.1887	$C_{17}H_{34}N_3O_6S_2$	0.3	31.1	2.5
201			12.3			440.1887	$C_{20}H_{30}N_3O_6S$	3.7	13.7	7.5
202			13.3			453.1678	$C_{16}H_{29}N_4O_9S$	2.8	51.2	4.5
203			18.7			465.1681	$C_{17}H_{29}N_4O_9S$	3.2	48.9	5.5
204				15.8		365.1074	$C_{19}H_{17}N_4O_2S$	0.7	56.4	13.5
205			33.0			365.1427	$C_{20}H_{21}N_4OS$	0.4	60.0	12.5
206			8.7			407.1887	$C_{20}H_{31}N_4OS_2$	4.7	87.0	7.5
207			13.3			415.2117	$C_{22}H_{31}N_4O_2S$	4.5	5.1	9.5
208			13.3			437.1948	$C_{22}H_{33}N_2O_3S_2$	2.1	43.0	7.5
209			12.3			440.1887	$C_{22}H_{34}NO_4S_2$	3.7	24.9	6.5
210			8.7			407.1887	$C_{23}H_{27}N_4OS$	1.3	84.4	12.5
211				23.7		467.1114	$C_{24}H_{23}N_2O_4S_2$	2.0	63.0	14.5
212			33.0			463.2266	$C_{24}H_{35}N_2O_5S$	0.5	48.3	8.5
213			12.3			440.1887	$C_{25}H_{30}NO_4S$	0.3	15.1	11.5
214				19.1		579.2923	$C_{25}H_{47}N_4O_7S_2$	4.2	32.3	4.5
215				19.1		579.2923	$C_{30}H_{47}N_2O_5S_2$	0.2	38.4	8.5
216				19.1		579.2923	$C_{33}H_{43}N_2O_5S$	3.6	33.6	13.5
217			31.1			659.2909	$C_{33}H_{47}N_4O_6S_2$	2.3	46.7	12.5
218			31.1			659.2909	$C_{36}H_{43}N_4O_6S$	1.1	28.1	17.5
219			31.1			659.2909	$C_{40}H_{43}N_4OS_2$	3.6	58.7	21.5
220			31.1			659.2909	$C_{41}H_{43}N_2O_4S$	3.0	37.6	21.5
221			13.3			453.1678	$C_{22}H_{25}N_6O_3S$	2.6	55.2	13.5
222			12.5			440.1892	$C_{18}H_{30}N_7O_2S_2$	0.5	61.9	7.5

and $[C_{12}H_{28}NO_2]^+$ (at 16.4 and 33.0 min, respectively); amines with unsaturated chain (rdb < 3.5) also appeared, for example, $[C_8H_{16}NS]^+$ (at 11.7 min in Fig. 3a), $[C_8H_{16}NO]^+$ (at 10.6 min, in Fig. 3b) and $[C_9H_{20}NO]^+$ (at 7.7 min in Fig. 3c); Ions with rdb = 3.5, like $[C_8H_{12}NO]^+$, $[C_{11}H_{18}N]^+$ (at 9.8 min and 17.3 min in Fig. 3b, separately) and $[C_{11}H_{18}NO]^+$ (at 7.7 min in Fig. 3c), probably were alkoxylated-anilines/pyridines; $[C_{11}H_{16}NS]^+$ and $[C_{12}H_{18}NS]^+$ (at 16.4 min and 21.2 min in Fig. 3a, b separately), with rdb = 4.5, may contain an aromatic ring with substituent group; $[C_{12}H_{16}NS]^+$ (at 16.4 min in Fig. 3a) with rdb = 5.5 may consist of an

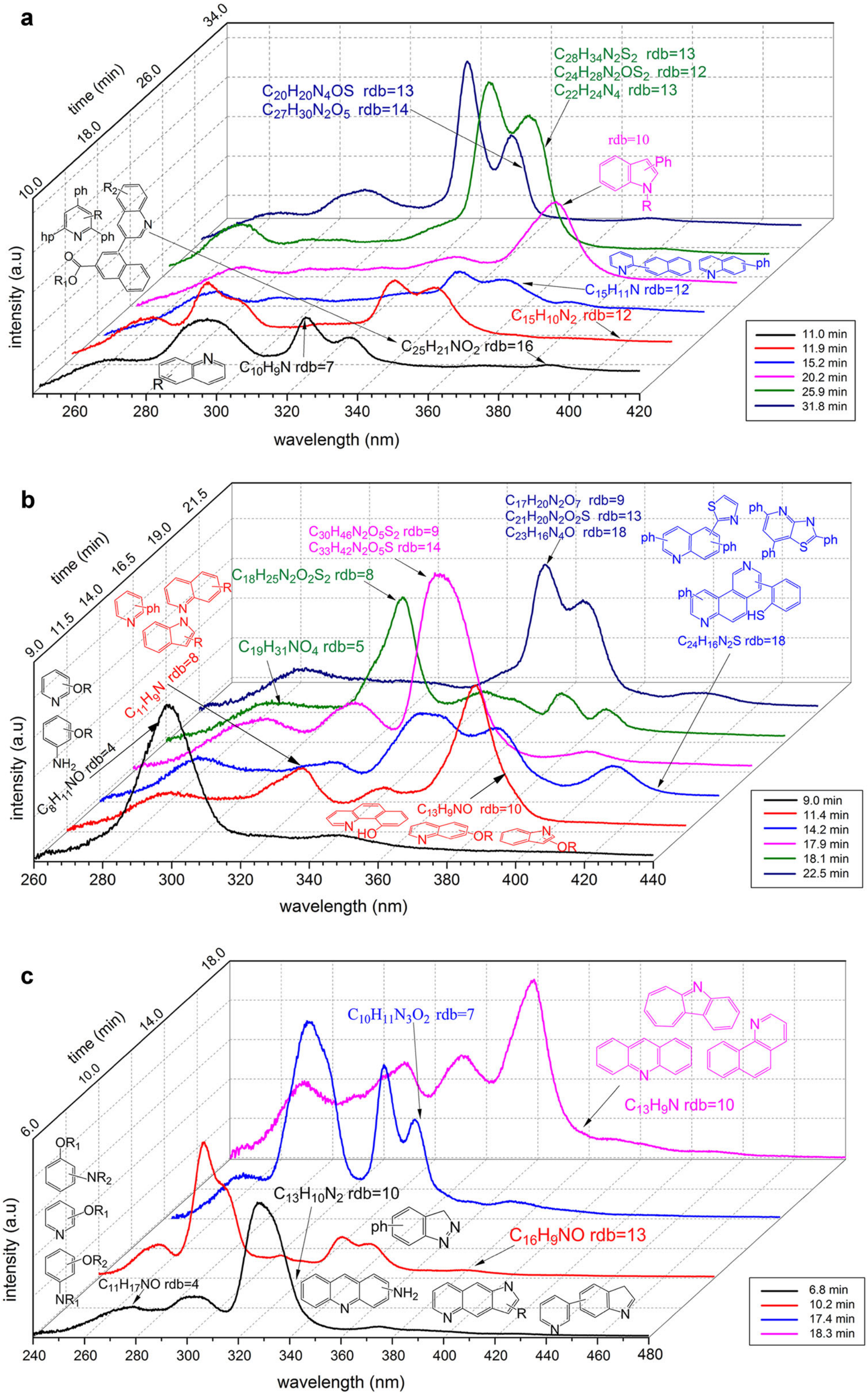

Fig. 4 Fluorescence spectra of fraction a (**a**), fraction b (**b**) and fraction c (**c**) (Time in labels referred to the moment when the FL spectrometer began to scan at 240 nm at a rate of 240 nm/min. Furthermore, it took the compound 0.75 min from FL detector to MS detector. Besides, the ph referred to phenyl)

Table 2 Isomeric compounds detected in Fig. 2 and Fig. 3

No.	Ion formula [M + H]+	Meas. *m/z*	Experimental *m/z*	|err| [mDa]	mSigma	rdb	Retention time (min)	Detected in figures
1	$C_9H_{23}N_2O_2$	191.1733	191.1754	2.1	14.9	−0.5	13.1	2a
2	$C_9H_{23}N_2O_2$	191.1739	191.1754	1.6	16.0	−0.5	13.2	2a
3	$C_9H_{23}N_2O_2$	191.1732	191.1754	2.3	35.9	−0.5	13.5	2a
4	$C_{13}H_{13}N_2O$	213.1068	213.1022	4.5	7.4	8.5	14.6	2a
5	$C_{13}H_{13}N_2O$	213.1066	213.1022	4.4	4.5	8.5	15.7	2a
6	$C_{18}H_{39}N_4$	311.3185	311.3169	1.6	13.0	1.5	17.5	2a
7	$C_{18}H_{39}N_4$	311.3165	311.3169	0.5	24.7	1.5	18.0	2a
8	$C_{18}H_{39}N_4$	311.3178	311.3169	0.9	15.2	1.5	18.2	2a
9	$C_{18}H_{39}N_4$	311.3170	311.3169	0.1	15.5	1.5	18.6	2a
10	$C_{25}H_{50}NO_2$	396.3811	396.3836	2.5	72.7	1.5	23.5	2a
11	$C_{25}H_{50}NO_2$	396.3813	396.3836	2.3	79.0	1.5	24.0	2a
12	$C_{25}H_{49}N_4O$	421.3910	421.3901	0.9	13.1	3.5	20.9	2a
13	$C_{25}H_{49}N_4O$	421.3904	421.3901	0.3	17.2	3.5	21.1	2a
14	$C_{25}H_{49}N_4O$	421.3915	421.3901	1.4	12.0	3.5	21.2	2a
15	$C_{13}H_{12}N$	182.0947	182.0964	1.8	7.8	8.5	19.3	2b
16	$C_{13}H_{12}N$	182.0948	182.0964	1.7	10.0	8.5	19.7	2b
17	$C_{13}H_{12}N$	182.0954	182.0964	1.0	2.3	8.5	19.9	2b
18	$C_{14}H_{17}N_2O_2$	245.1265	245.1285	2.0	32.2	7.5	24.6	2b
19	$C_{14}H_{17}N_2O_2$	245.1296	245.1285	1.2	41.0	7.5	24.8	2b
20	$C_{14}H_{17}N_2O_2$	245.1298	245.1285	1.4	54.4	7.5	24.9	2b
21	$C_{10}H_{10}N$	144.0819	144.0808	1.2	29.3	6.5	12.3	3a
22	$C_{10}H_{10}N$	144.0822	144.0808	1.4	10.1	6.5	12.5	3a
23	$C_{10}H_{10}N$	144.0826	144.0808	1.8	19.9	6.5	13.3	3a
24	$C_{11}H_{12}N$	158.0984	158.0964	2.0	16.6	6.5	11.7	3a
25	$C_{11}H_{12}N$	158.0977	158.0964	1.3	19.5	6.5	14.0	3a
26	$C_{11}H_{12}N$	158.0972	158.0964	0.8	14.3	6.5	16.4	3a
27	$C_8H_{16}NS$	158.0984	158.0998	1.4	15.1	1.5	11.7	3a
28	$C_8H_{16}NS$	158.0977	158.0998	2.1	28.9	1.5	14.0	3a
29	$C_8H_{16}NS$	158.0972	158.0998	2.6	28.4	1.5	16.4	3a
30	$C_{12}H_{12}N$	170.0959	170.0964	0.5	96.5	7.5	11.7	3a
31	$C_{12}H_{12}N$	170.0959	170.0964	0.5	96.5	7.5	14.0	3a
32	$C_{12}H_{12}N$	170.0961	170.0964	0.3	14.1	7.5	14.7	3a
33	$C_{11}H_{16}NS$	194.0985	194.0998	1.2	46.3	4.5	16.4	3a
34	$C_{11}H_{16}NS$	194.0971	194.0998	2.7	40.6	4.5	17.1	3a
35	$C_{11}H_{16}NS$	194.0969	194.0998	2.9	34.5	4.5	18.2	3a
36	$C_{11}H_{16}NS$	194.0975	194.0998	2.3	46.0	4.5	18.7	3a
37	$C_{11}H_{16}NS$	194.0980	194.0998	1.8	58.0	4.5	21.4	3a
38	$C_{13}H_{16}NS$	218.0977	218.0998	2.1	32.5	6.5	18.2	3a
39	$C_{13}H_{16}NS$	218.0986	218.0998	1.2	93.9	6.5	18.7	3a
40	$C_{13}H_{16}NS$	218.0982	218.0998	1.5	33.0	6.5	21.4	3a
41	$C_{23}H_{19}N_2S$	355.1301	355.1263	3.8	40.9	15.5	17.1	3a
42	$C_{23}H_{19}N_2S$	355.1308	355.1263	4.4	42.8	15.5	18.2	3a
43	$C_6H_{12}NS$	130.0670	130.0685	1.5	41.3	1.5	11.4	3b
44	$C_6H_{12}NS$	130.0666	130.0685	1.9	38.4	1.5	12.2	3b
45	$C_7H_{14}NS$	144.0826	144.0841	1.6	28.4	1.5	12.2	3b
46	$C_7H_{14}NS$	144.0829	144.0841	1.3	32.8	1.5	12.7	3b
47	$C_7H_{14}NS$	144.0821	144.0841	2.0	18.0	1.5	14.1	3b
48	$C_{12}H_{14}N$	172.1120	172.1121	0.1	16.3	6.5	15.8	3b

Table 2 continued

No.	Ion formula [M + H]+	Meas. *m/z*	Experimental *m/z*	|err| [mDa]	mSigma	rdb	Retention time (min)	Detected in figures
49	$C_{12}H_{14}N$	172.1120	172.1121	0.1	17.9	6.5	16.4	3b
50	$C_{12}H_{14}N$	172.1124	172.1121	0.3	20.5	6.5	17.3	3b
51	$C_{12}H_{14}N$	172.1123	172.1121	0.2	16.2	6.5	19.1	3b
52	$C_{12}H_{14}N$	172.1131	172.1121	1.0	82.8	6.5	21.2	3b
53	$C_9H_{13}N_2S$	181.0833	181.0794	3.9	32.1	4.5	10.0	3b
54	$C_9H_{13}N_2S$	181.0836	181.0794	4.2	24.3	4.5	10.9	3b
55	$C_9H_{13}N_2S$	181.0824	181.0794	3.0	18.0	4.5	11.4	3b
56	$C_{14}H_{12}N$	194.0967	194.0964	0.3	48.3	9.5	16.4	3b
57	$C_{14}H_{12}N$	194.0968	194.0964	0.4	24.0	9.5	17.3	3b
58	$C_{14}H_{12}N$	194.0969	194.0964	0.5	63.8	9.5	18.3	3b
59	$C_{14}H_{12}N$	194.0968	194.0964	0.4	39.4	9.5	19.1	3b
60	$C_{14}H_{12}N$	194.0966	194.0964	0.1	29.3	9.5	21.2	3b
61	$C_{13}H_{10}N$	180.0820	180.0808	1.3	22.8	9.5	14.9	3c
62	$C_{13}H_{10}N$	180.0816	180.0808	0.8	1.8	9.5	15.6	3c
63	$C_{13}H_{10}N$	180.0817	180.0808	0.9	7.8	9.5	15.7	3c
64	$C_{13}H_{10}N$	180.0818	180.0808	1.0	18.1	9.5	18.5	3c
65	$C_{13}H_{10}N$	180.0815	180.0808	0.7	5.8	9.5	19.7	3c
66	$C_{10}H_{14}NS$	180.0820	180.0841	2.1	8.3	4.5	14.9	3c
67	$C_{10}H_{14}NS$	180.0816	180.0841	2.6	32.9	4.5	15.6	3c
68	$C_{10}H_{14}NS$	180.0817	180.0841	2.5	20.3	4.5	15.7	3c
69	$C_{10}H_{14}NS$	180.0818	180.0841	2.4	29.9	4.5	18.5	3c
70	$C_{10}H_{14}NS$	180.0815	180.0841	2.7	32.3	4.5	19.7	3c
71	$C_{18}H_{17}N_2$	261.1368	261.1386	1.8	54.1	11.5	14.9	3c
72	$C_{18}H_{17}N_2$	261.1362	261.1386	2.5	11.6	11.5	15.6	3c
73	$C_{18}H_{17}N_2$	261.1367	261.1386	1.9	56.1	11.5	15.7	3c
74	$C_{19}H_{17}N_4$	301.1435	301.1447	1.1	6.1	13.5	14.2	3c
75	$C_{19}H_{17}N_4$	301.1440	301.1447	0.8	20.9	13.5	15.1	3c

aromatic ring and unsaturated groups and/or aliphatic rings. Ions with rdb = 6.5, like $[C_{10}H_{10}N]^+$, $[C_{11}H_{12}N]^+$ (at 12.5 and 16.4 min in Fig. 3a, respectively) and $[C_{12}H_{14}N]^+$ (at 15.8 min in Fig. 3b), contained quinolone rings possibly.

In $N_1O_\alpha S_\gamma$ ($\alpha + \gamma \leq 2$) group, the molecular structure became more complex with rdb bigger than 7.5, it may contain a phenylpyridine ring/quinoline ring/amine ring/an indole ring plus an unsaturated alkyl/aliphatic ring/ester/carbonyl group. For instance, ions with rdb = 7.5, like $[C_{13}H_{14}N]^+$ (at 16.7 min, in Fig. 2b), $[C_{12}H_{12}N]^+$ (at 14.0 min in Fig. 3a) and $[C_{11}H_{10}N]^+$ (at 12.7 min in Fig. 3b), may contain a phenhylpyridine/quinolone/aniline ring. For species with rdb = 8.5, $[C_{12}H_{10}N]^+$, $[C_{13}H_{12}N]^+$ and $[C_{14}H_{14}N]^+$ (at 18.5, 19.9 and 20.9 min, in Fig. 2b, respectively) may consist of an indenopyridine ring/carbazole ring/benzindole ring, besides an aniline ring and phenhylpyridine ring. For species with rdb $\geq$ 9.5, benzoquinoline/acridine/benzocarbazole may exist, for example, $[C_{17}H_{12}NO]^+$ (at 14.3 min in Fig. 2a), $[C_{15}H_{10}N]^+$ (at 21.8 min in Fig. 2b), $[C_{25}H_{22}NO_2]^+$ (at 12.5 min in Fig. 3a), $[C_{15}H_{12}N]^+$ (at 16.4 min in Fig. 3a), $[C_{13}H_{10}NO]^+$ (at 12.7 min in Fig. 3b), $[C_{13}H_{10}N]^+$ (at 19.7 min in Fig. 3c)and so on.

CWSFS could confirm partial conjecture by rdb. Figure 4a presented the fluorescence spectra of fraction a separated by HPLC. There was moderate intensity fluorescence at 330 nm and 360 nm respectively due to $C_{10}H_9N$ and $C_{15}H_{11}N$, indicating they had a double-ringed aromatic and three aromatic structures. The weak intensity fluorescence was around 410 nm caused by $C_{25}H_{21}NO_2$ because of its four aromatic rings. All of their ions sturctures ($[C_{10}H_{10}N]^+$ with rdb = 6.5, $[C_{15}H_{12}N]^+$ with rdb = 11.5 and $[C_{25}H_{22}NO_2]^+$ with rdb = 15.5) were supposed above shown in Fig. 4a, proving that CWSFS result was consist with rdb conjecture. Figure 4b showed the fluorescence spectra of fraction b separated by HPLC. $C_8H_{11}NO$, $C_{11}H_9N$, $C_{13}H_9NO$ had obvious fluorescence at 298 nm, 331 nm, 379 nm, due to structures of a single-

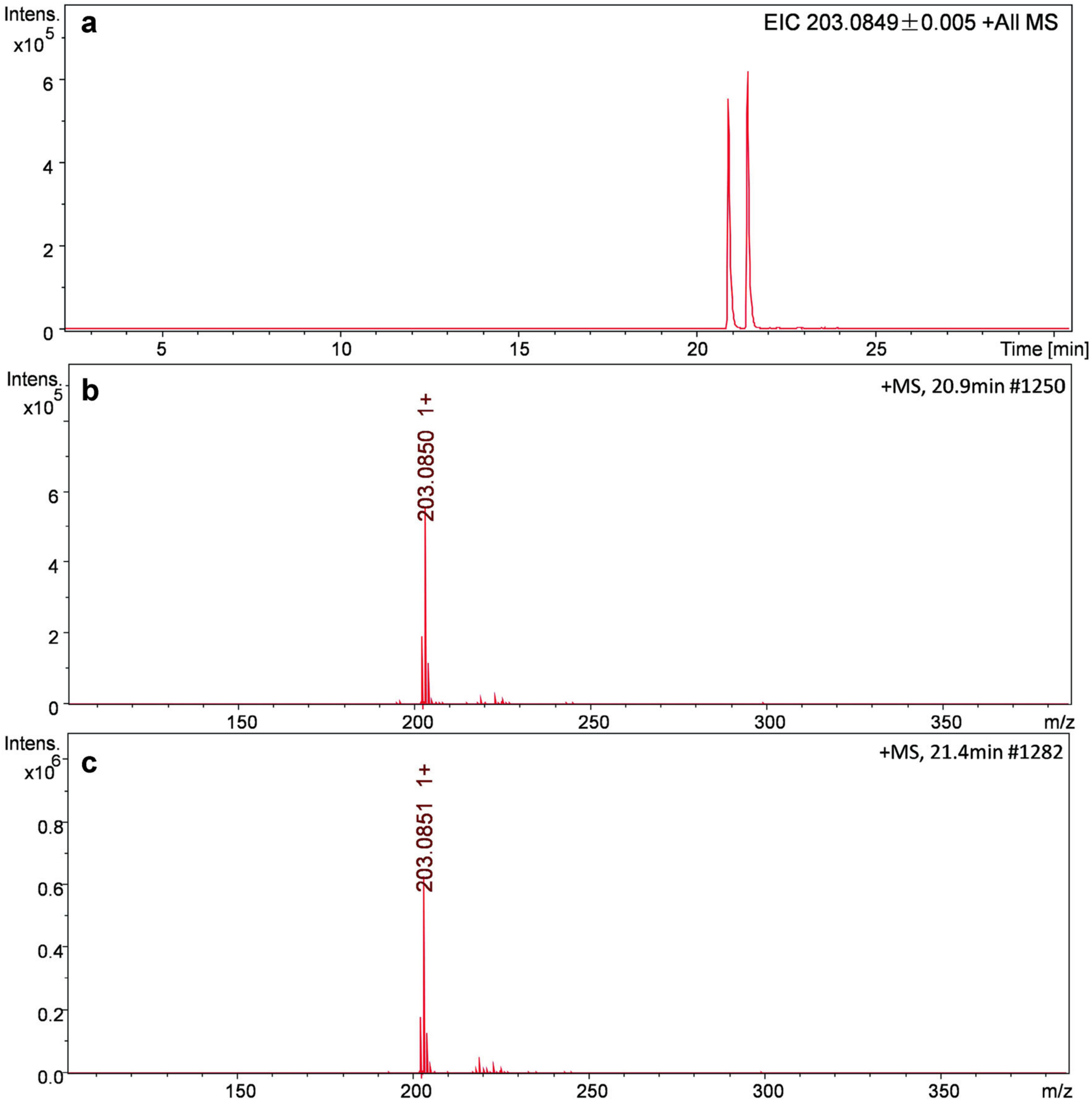

Fig. 5 EIC (**a**) and mass spectra (**b** and **c**) of isomers of $[C_{11}H_{11}N_2O_2]^+$ (*m*/*z* = 203.0849) detected by GC-APCI-MS

ringed aromatic, double-ringed aromatic, and three aromatic rings, respectively. These were also corresponding to the conjecture by rdb mentioned before. Besides that, $C_{11}H_{17}NO$, $C_{13}H_9N$ had strong fluorescence around 280 nm and 370 nm in Fig. 4c, separately, corresponding to single aromatic ring and three aromatic rings. These verified the alkoxylated-aniline/pyridine structures inferred by rdb = 3.5 of $[C_{11}H_{18}NO]^+$ and benzoquinoline/acridine/cycloheptaindole structures with rdb = 9.5 of $[C_{13}H_{10}N]^+$.

However, most of arylamines and 2-hydroxyquinoline (C_9H_7NO) cannot be effectively ionized and detected under the positive ion mode because of its relative weak basicity caused by hyperconjugation or the presence and position of the hydroxy group (Hughey et al. 2001; da Silva et al. 2014).

In $N_1O_\alpha S_\gamma$ ($\alpha + \gamma = 3$–4) group, it became complex, structures could not be proposed just by rdb, and CWSFS could be informative sometimes. For example, $[C_{20}H_{32}NO_2S_2]^+$ (peak 5 at 13.3 min in Fig. 3a), with rdb = 5.5, may be unsaturated ketones, but it fluoresced at 290 nm indicated that it was aromatic structure.

In N_2 group, the species with rdb = 4.5, like $[C_{20}H_{35}N_2]^+$ appeared at 21.6 min in Fig. 2a, may be a pyridine or an aniline with an amino group, unsaturated amine was also possible. The proposed structure of compound with rdb = 5.5 ($[C_{35}H_{63}N_2]^+$ at 21.4 min in Fig. 2a,) was indole or a pyridine or an aniline with an amino group as well as alkylated-benzimidazole. With rdb from 6.5 (as $[C_{23}H_{37}N_2]^+$ at 10.3 min in Fig. 2a) to 12.5 (as $[C_{18}H_{15}N_2]^+$ at 25.2 min in Fig. 2b), pyrrolic and pyridine rings may exist.

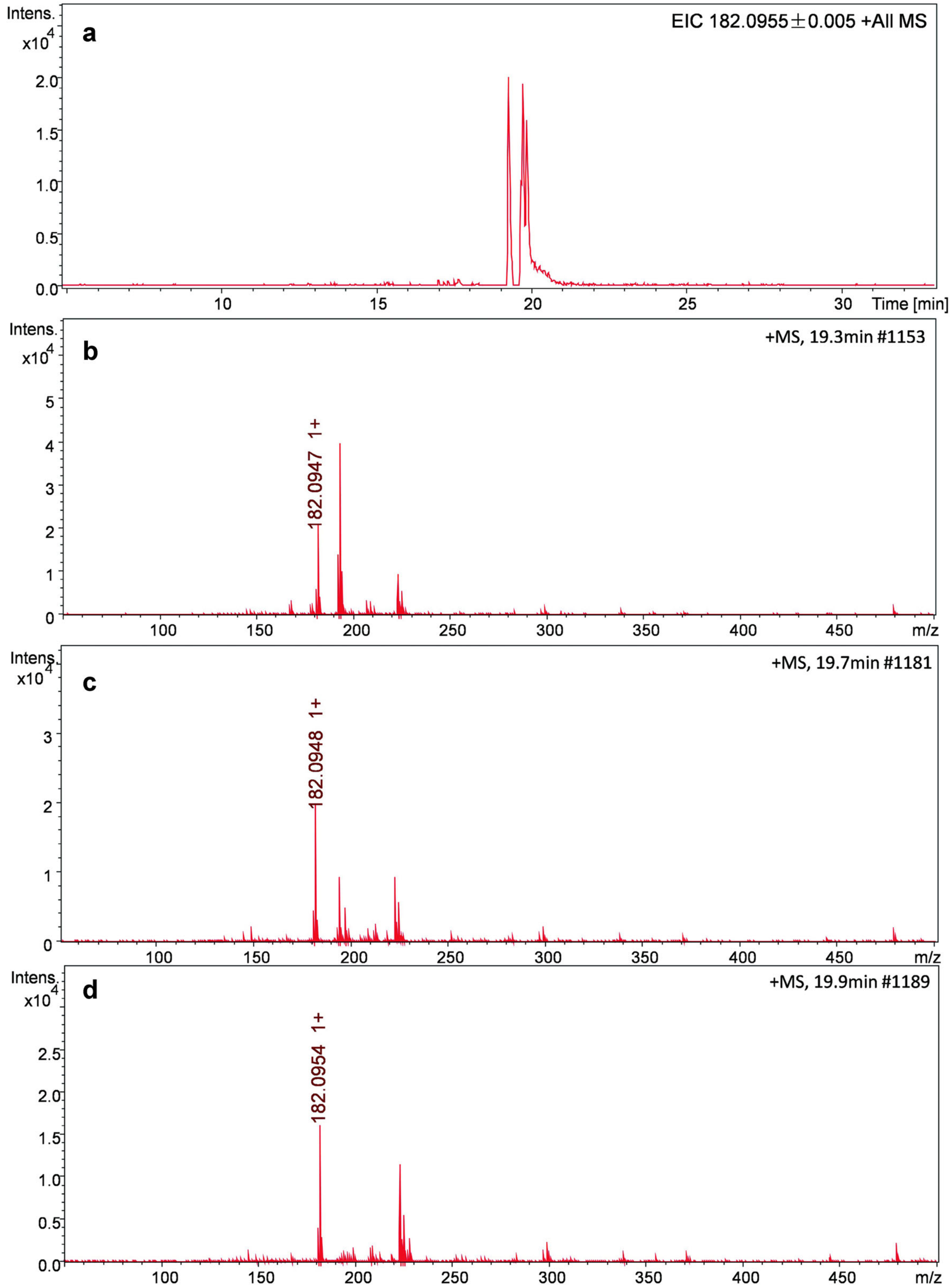

Fig. 6 EIC (**a**) and mass spectra (**b** and **c**) of isomers of $[C_{13}H_{12}N]^+$ ($m/z = 182.0955$) detected by GC-APCI-MS

Moreover, in $N_2O_\alpha S_\gamma$ ($\alpha + \gamma \leq 3$) group, series of species with rdb < 4.5 may have two amino groups, for example, $[C_7H_{19}N_2O_2]^+$, $[C_9H_{23}N_2O_2]^+$ and $[C_{18}H_{41}N_2O_3]^+$ (at 10.3, 13.1 and 21.6 min in Fig. 2a, separately), all with rdb = −0.5, may be saturated aliphatic amines. Species with rdb > 8.5 may contain a benzoquinoline or acridine ring

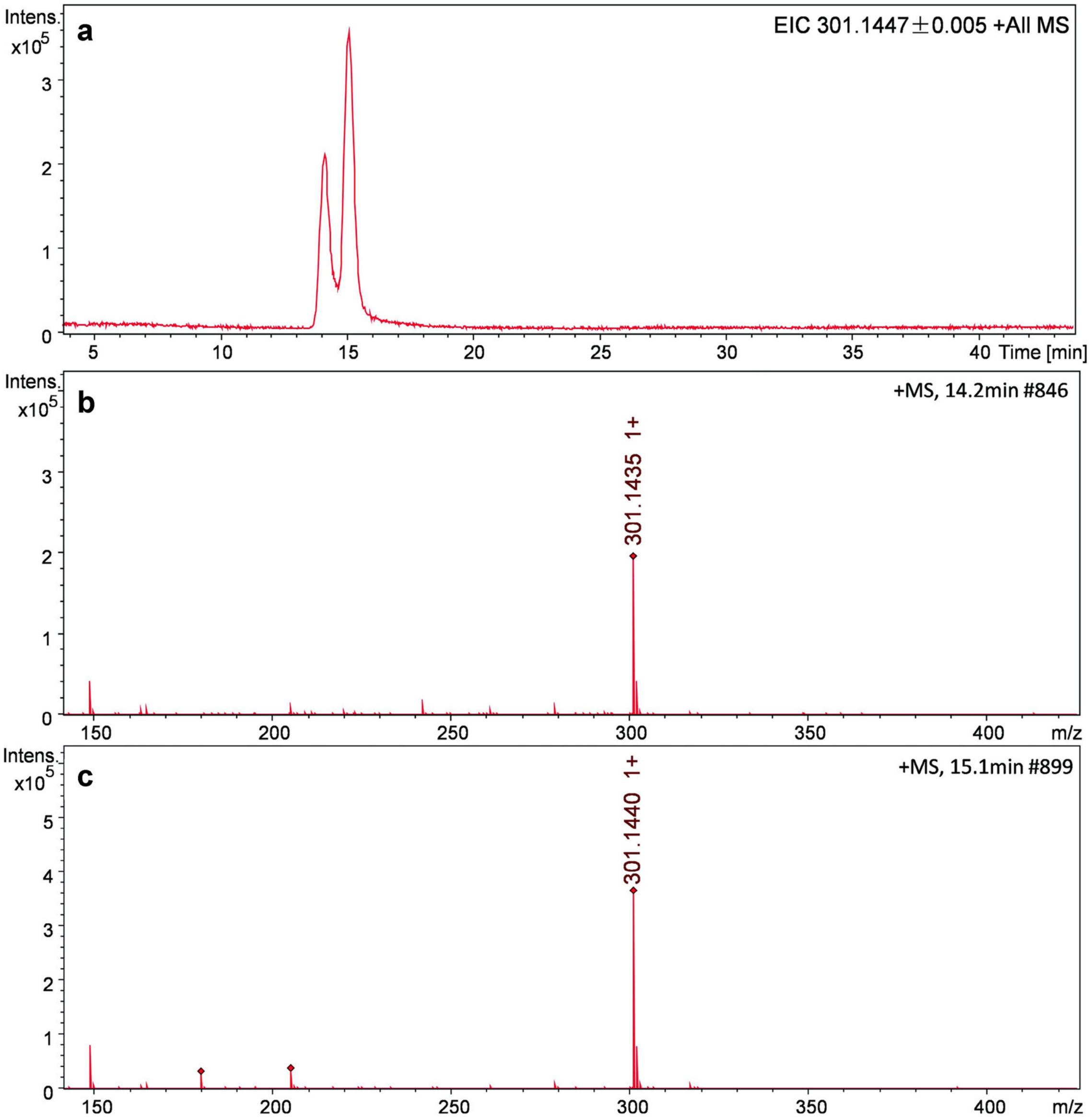

Fig. 7 EIC (**a**) and mass spectra (**b** and **c**) of isomers of $[C_{19}H_{17}N_4]^+$ ($m/z = 301.1447$) detected by HPLC–ESI–MS

with an amino group besides quinoline and indole rings connected by a bridged bond, for example, $[C_{25}H_{22}NO_2]^+$ (at 12.5 min in Fig. 3a) with rdb = 15.5 may consists of phenyls-pyridines or ester-quinoline and so on, estimating $C_{25}H_{21}NO_2$ fluoresced at longer than 400 nm shown in Fig. 4a.

As shown in Table 1, $N_\beta O_\alpha S_\gamma$ ($\beta = 3$–5, $\alpha + \gamma = 0$–10) had rdb values from 1.5 to 21.5. Since the minimal rdb number for $[M + H]^+$ of an aromatic ring is 3.5, aliphatic amine compounds existed, like $[C_{18}H_{39}N_4]^+$ (rdb = 1.5, at 17.5 min in Fig. 2a).

Possible structures of partial compounds comprehensively analyzed by rdb and fluorescence spectra were exhibited in Fig. 4. In addition, lower fluorescence intensity was observed when the wavelength was longer than 420 nm in Fig. 4. Since the intensity area was proportional to the concentration of the sample in diluted solution, this indicated that the compounds mainly had less than four aromatic rings. This is applied to compare among similar compounds (as is the case on N-compounds) in the same conditions.

4.2 Isomers

This work combined chromatography with MS to separate and analyze isomers since TOF-MS could not distinguish isomers. The existence of isomers was confirmed by the apparent difference in retention time shown in Table 2 and several clean mass spectra of isomers were presented in Fig. 5. Retention times of isomers are dependent on the

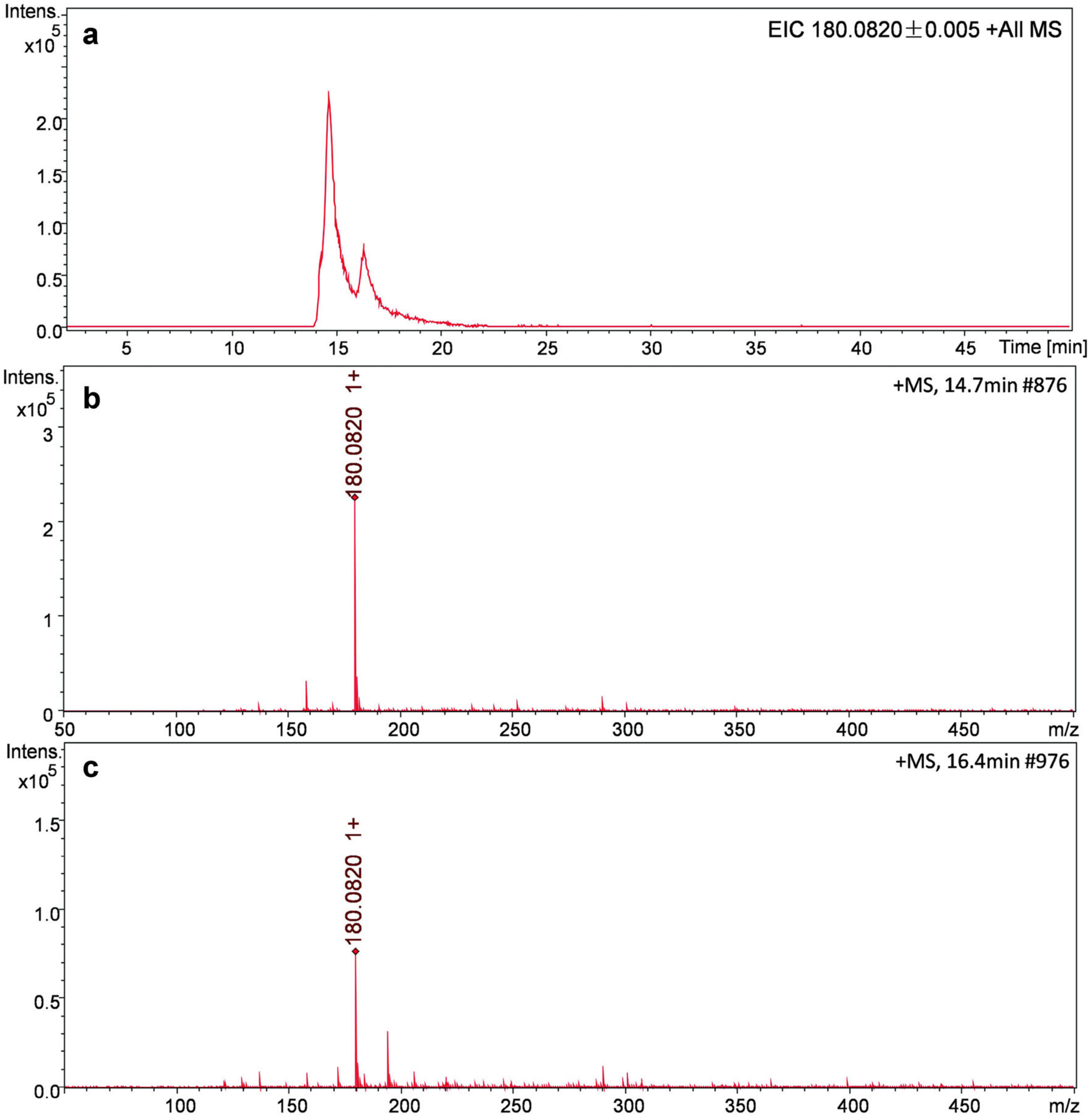

Fig. 8 EIC (**a**) and mass spectra (**b** and **c**) of isomers of $[C_{13}H_{10}N]^+$ (m/z = 180.0820) detected by HPLC–ESI–MS

strength of reversible intermolecular forces of functional groups, molecular spatial structures, partition coefficient between stationary phase and mobile phase. Moreover, volatilities and polarities of isomers also played a major role in GC and HPLC separation, respectively (da Silva et al. 2014).

Identification of the target peaks of isomers can be simplified by using of extracted ion chromatograms (EIC). Figure 5 shown two chromatographic peaks of $[C_{11}H_{11}N_2O_2]^+$ (m/z = 203.0849) detected by GC-APCI MS, indicating the existence of isomers at 20.9 min and 21.4 min. Since the rdb number of $C_{11}H_{10}N_2O_2$ is 8, one of the possible chemical structures may be a quinoline plus various alkyl groups. Such alkyl groups with various structures induced the difference in volatilities and retention time. For another instance, Fig. 6 presented three isomers of $C_{13}H_{11}N$ separated by GC.

Methanol, as the mobile phase, has high adsorption effects on the NPAC due to the interactions induced by hydrogen bonds O–H···N and O–H···π. Thus compounds with low polarity have long retention times in HPLC (Xia et al. 2016). For example, Fig. 7 presented two chromatographic peaks of $[C_{19}H_{17}N_4]^+$ (m/z = 301.1447) detected by HPLC–ESI–MS, the isomers appearing at 14.2 min and 15.1 min. The possible structures of $[C_{19}H_{17}N_4]^+$ (rdb = 13.5) may contain carbazole/phenylaniline/phenylpyrimidine and so on. Thus isomeric compounds with different polarities led to flow out in HPLC in turn. $C_{13}H_9N$ also had two isomers shown in Fig. 8.

However, specific isomer structural assignment is not obtained here. We could not get the exact position of functional groups in the aromatic chain by mass spectra. For example, it is not sure that $C_{13}H_9N$ is benzoquinoline or acridine or phenanthridine, and so on. It proposes target for following work.

5 Conclusion

N-containing compounds were extracted from asphaltene that was produced by co-processing coal tar and oil reside and purified by Soxhlet extraction. It is proven to be an effective approach for separation and detailed characterization of three distillates of N-containing compounds by GC-APCI-Q-TOF MS and HPLC-FL-ESI-Q-TOF-MS analysis. More than two hundred N-compounds were tentatively identified, most of them contain N-polyaromatic aromatic rings, including pyridines, pyrroles, anilines, quinolones, carbazoles and indoles for $N_\beta O_\alpha S_\gamma$ ($\beta = 1$–2) class. In $N_{fig\beta}O_\alpha S_\gamma$ ($\beta = 3$–5) class, aliphatic amine may exist. CWSFS indicated structures of two or three aromatic rings were the majority of NPAC. Possible structures of partial compounds were proposed by comprehensive analysis of rdb and fluorescence spectra. Some isomers were separated. Characterization of the chemical compositions of NPAC in asphaltene should be beneficial to nitrogen removal and the effectively application.

Acknowledgements The authors gratefully acknowledge the financial support of this work by the National Natural Science Foundation of China (No. U1510122). The authors declare that the experiments comply with the current laws of China.

Compliance with ethical standards

Conflict of interest The authors declare that they have no conflict of interest

References

Abdallah WA, Yang Y (2012) Raman spectrum of asphaltene. Energy Fuels 26:6888–6896. doi:10.1021/ef301247n

Ares AM, Gonzalez Y, Nozal MJ, Bernal JL, Higes M, Bernal J (2015) Development and validation of a liquid chromatography with mass spectrometry method to determine resveratrol and piceid isomers in beeswax. J Sep Sci 38:197–204. doi:10.1002/jssc.201400955

Barman BN, Cebolla VL, Mehrotra AK, Mansfield CT (2001) Petroleum and coal. Anal Chem 73:2791–2803

Beens J, Blomberg J, Schoenmakers PJ (2000) Proper tuning of comprehensive two-dimensional gas chromatography (GC × GC) to optimize the separation of complex oil fractions. HRC J High Res Chrom 23:182–188

da Silva JM, Machado ME, Maciel GP, Dal Molin D, Caramao EB (2014) Speciation of nitrogen-containing compounds in an unfractionated coal tar sample by comprehensive two-dimensional gas chromatography coupled to time-of-flight mass spectrometry. J Chromatogr A 1373:159–168. doi:10.1016/j.chroma.2014.11.004

Gargiulo V, Apicella B, Stanzione F, Tregrossi A, Milian M, Ciajolo A, Russo C (2016) Structural characterization of large polycyclic aromatic hydrocarbons. Part 2: Solvent-separated fractions of coal tar pitch and naphthalene-derived pitch. Energy Fuels 30:2574–2583. doi:10.1021/acs.energyfuels.5b02576

George A, Morgan TJ, Alvarez P, Millan M, Herod AA, Kandiyoti R (2010) Fractionation of a coal tar pitch by ultra-filtration, and characterization by size exclusion chromatography, UV-fluorescence and laser desorption-mass spectroscopy. Fuel 89:2953–2970. doi:10.1016/j.fuel.2010.04.011

Goncalves S, Castillo J, Fernández A, Hung J (2004) Absorbance and fluorescence spectroscopy on the aggregation behavior of asphaltene–toluene solutions. Fuel 83:1823–1828. doi:10.1016/j.fuel.2004.03.009

Hughey CA, Hendrickson CL, Rodgers RP, Marshall AG (2001) Elemental composition analysis of processed and unprocessed diesel fuel by electrospray ionization fourier transform ion cyclotron resonance mass spectrometry. Energy Fuels 15:1186–1193. doi:10.1021/ef010028b

Li KJ et al (2015) Further insights into the structure and chemistry of the Gilsonite asphaltene from a combined theoretical and experimental approach. Fuel 157:16–20. doi:10.1016/j.fuel.2015.04.029

Matzke M, Jess A, Litzow U (2015) Polar nitrogen-containing aromatic compounds as carriers of natural diesel lubricity. Fuel 140:770–777. doi:10.1016/j.fuel.2014.09.037

McKenna AM et al (2013) Heavy petroleum composition. 3. Asphaltene aggregation. Energy Fuels 27:1246–1256. doi:10.1021/ef3018578

Michels R, Langlois E, Ruau O, Mansuy L, Elie M, Landais P (1996) Evolution of asphaltenes during artificial maturation: a record of the chemical processes. Energy Fuels 10:39–48. doi:10.1021/ef9501410

Mullins OC et al (2012) Advances in asphaltene science and the yen-mullins model. Energy Fuels 26:3986

Pereira TMC et al (2014) FT-ICR MS analysis of asphaltenes: asphaltenes go in, fullerenes come out. Fuel 131:49–58. doi:10.1016/j.fuel.2014.04.049

Plater MJ, Jackson T (2003) Polyaromatic amines. Part 3: Synthesis of poly(diarylamino)styrenes and related compounds. Tetrahedron 59:4673–4685. doi:10.1016/S0040-4020(03)00520-9

Smith DR, Robb DB, Blades MW (2009) Comparison of dopants for charge exchange ionization of nonpolar polycyclic aromatic hydrocarbons with reversed-phase LC-APPI-MS. J Am Soc Mass Spectrom 20:73–79. doi:10.1016/j.jasms.2008.09.012

Wang ZC et al (2013) Study on the structure and association of asphaltene derived from liquefaction of lignite by fluorescence spectroscopy. Fuel 109:94–100. doi:10.1016/j.fuel.2012.12.011

Wu HC, Kessler MR (2015) Asphaltene: structural characterization, molecular functionalization, and application as a low-cost filler in epoxy composites. RSC Adv 5:24264–24273. doi:10.1039/c5ra00509d

Wu MM, Yang JL, Zhang YZ (2012) Comparison study of modified asphalt by different coal liquefaction residues and different preparation methods. Fuel 100:66–72. doi:10.1016/j.fuel.2011.12.042

Xia JL, Fan X, You CY, Wei XY, Zhao YP, Cao JP (2016) Sequential ultrasonic extraction of a Chinese coal and characterization of nitrogen-containing compounds in the extracts using high-performance liquid chromatography with mass spectrometry. J Sep Sci 39:2491–2498. doi:10.1002/jssc.201600190

Xu CG et al (2013) Synthesis of graphene from asphaltene molecules adsorbed on vermiculite layers. Carbon 62:213–221. doi:10.1016/j.carbon.2013.05.059

Ying S, Jian L, Bo LW, Su ZX (2009) Preparation of mesophase pitch using coal lique fraction residue. J China Coal Soc 34:1125–1128

You CY et al (2015) Molecular characteristics of a Chinese coal analyzed using mass spectrometry with various ionization modes. Fuel 155:122–127. doi:10.1016/j.fuel.2015.04.009

Zhang L, Yang JL, Zhu JS, Liu ZY, Li BQ, Hu TD, Dong BZ (2002) Properties and liquefaction activities of ferrous sulfate based catalyst impregnated on two Chinese bituminous coals. Fuel 81:951–958. doi:10.1016/S0016-2361(02)00008-X

Zubkova V (2011) Chromatographic methods and techniques used in studies of coals, their progenitors and coal-derived materials. Anal Bioanal Chem 399:3193–3209. doi:10.1007/s00216-010-4328-x